JOURNAL OF MATERIALS SCIENCE 20 (1985) 3873–3880

Crazing and shear deformation in glass bead-filled glassy polymers

M. E. J. DEKKERS*, D. HEIKENS
Eindhoven University of Technology, Laboratory of Polymer Technology, PO Box 513, 5600 MB Eindhoven, The Netherlands

The competition between craze formation and shear band formation at small glass beads embedded in matrices of glassy polymers has been investigated. This has been done by performing constant strain rate tensile tests over a wide range of strain rates and temperatures, and examining the deformation pattern formed at the beads with a light microscope. The glassy polymers under investigation were polystyrene, polycarbonate, and two types of styrene–acrylonitrile copolymer. It was found that besides matrix properties, strain rate and temperature, the degree of interfacial adhesion between the glass beads and the matrix also has a profound effect on the competition between craze and shear band formation: at excellently adhering beads craze formation is favoured, whereas at poorly adhering beads shear band formation is favoured. This effect is caused by the difference in local stress situation, craze formation being favoured under a triaxial stress state and shear band formation under a biaxial stress state. The kinetics of crazing and shear deformation have also been studied, using a simple model and Eyring's rate theory of plastic deformation. The results suggest that chain scission may be the rate-determining step in crazing but not in shear deformation.

1. Introduction

The tensile deformation of glassy polymers can be considered to be a competition between crazing and shear deformation [1–3]. If shear deformation is the dominant deformation process, the polymer is generally ductile. If crazing occurs preferentially the polymer is generally brittle, unless the growth of the crazes is controlled by dispersed particles as in rubber-toughened polystyrene. Crazing and localized shear deformation (shear bands) begin at heterogeneities because these give rise to inhomogeneous stress fields and thus act as stress concentrators. A glass bead is a well-defined heterogeneity and the three-dimensional stress situation around an isolated glass bead embedded in a polymer matrix can be computed quite accurately. Therefore the system of a glass bead embedded in a glassy polymer matrix is very suitable for studying crazing and shear deformation.

In recent studies the mechanisms for craze formation [4, 5] and shear band formation [6] were investigated at small glass beads (diameter about 30 μm) embedded in matrices of, respectively, polystyrene and polycarbonate which were subjected to uniaxial tension. These studies have provided a good insight into the three-dimensional stress situation required to start craze and shear band formation as well as into the effect of interfacial adhesion on the mechanisms for craze and shear band formation. In the case of an excellently adhering glass bead in a polystyrene matrix, the crazes form near the poles of the bead. Stress analysis shows that these are regions of maximum dilatation and of

Present address: General Electric Company, Research and Development Center, Polymer Physics Branch, PO Box 8, Schenectady, New York 12301, USA.

0022–2461/85 $03.00 + .12

maximum principal stress. At an excellently adhering glass bead in a polycarbonate matrix the shear bands form near the surface of the bead at 45° from the poles defined by the symmetry axis of the stressed sphere. These are regions of maximum principal shear stress and of maximum distortion strain energy density. In the case of poor interfacial adhesion between the glass bead and the matrix, both craze and shear band formation are preceded by dewetting along the interface between bead and matrix. At dewetting a curvilinear interfacial crack is formed, starting at the pole and propagating in the direction of the equator until, at an angle of about 60° from the pole, a craze or shear band originates at the tip of the interfacial crack.

The aim of the present work is to study the effect of matrix properties, deformation rate, temperature and degree of interfacial adhesion on the competition between craze and shear band formation at glass beads. For this purpose constant strain rate tensile tests have been performed with a number of glass bead-filled glassy polymers over a wide range of strain rates and temperatures. The kinetics of crazing and shear deformation are also studied, using a simple model and Eyring's rate theory of plastic deformation [7, 8]. This is done only with those glass bead-filled composites and under those test conditions for which it is well established that only one of the two possible deformation processes occurs.

2. Experimental details

The glassy polymers under investigation were:

1. polystyrene (PS): Styron 634 (Dow Chemical) with a glass transition temperature, T_g, of about 89° C;

2. polycarbonate (PC): Makrolon 2405 (Bayer), T_g about 137° C;

3. two types of styrene–acrylonitrile copolymer (SAN) containing different wt % of acrylonitrile (AN): SAN1: Tyril 790 (Dow Chemical) containing 30 wt % AN, T_g about 99° C; SAN2: obtained from Dow Chemical, containing 42.5 wt % AN, T_g about 108° C.

The glass beads used have a diameter range of 10 to 53 μm with an average diameter of 30 μm.

The glass bead-filled composites based on PS and PC were prepared as described elsewhere [4, 6]. The composites based on SAN were prepared in the same way as those based on PS. Excellent interfacial adhesion between the glass beads and SAN was obtained by treating the beads with a cationic vinylbenzyl trimethoxysilane (Dow Corning Z-6032). Poor interfacial adhesion was obtained with a silicone oil (Dow Corning DC-200).

The constant strain rate tensile tests were performed on a thermostatted Zwick tensile tester. Closed loop operation made accurate constant strain rate experiments possible. The dimensions of the tensile specimens used were chosen according to ASTM D 638 III.

The competition between craze formation and shear band formation at the glass beads was investigated by tensile testing specimens that contain only a very low percentage (about 0.5 vol %) of glass beads. As these specimens are transparent the deformation patterns, formed at the beads during the tensile test, can easily be observed with a light microscope afterwards. When fracture did not occur prior to yield, the tensile tests were stopped at the moment that the yield point was reached in order to exclude post-yield behaviour from the investigations. The tensile tests were performed over a strain rate range from 0.01 to 10 min^{-1} and a temperature range from room temperature to about 10° C below T_g.

3. Results and discussion

3.1. Competition between craze formation and shear band formation

3.1.1. PS

PS has been examined over the temperature range from 20 to 80° C and the strain range from 0.01 to 10 min^{-1}. Over this whole range, at both excellently and poorly adhering glass beads only crazes were observed; there was no visual indication of shear band formation at the beads.

3.1.2. PC

PC has been examined over the temperature range from 20 to 120° C and the strain rate range from 0.01 to 10 min^{-1}. Over this whole range, at both excellently and poorly adhering glass beads only shear bands were observed; there was no visual indication of craze formation at the beads.

3.1.3. SAN

Both SAN1 and SAN2 have been examined over the temperature range from 20 to 90° C and the strain rate range from 0.01 to 10 min^{-1}. In this

TABLE I Deformation pattern observed at excellently adhering glass beads in a SAN1 matrix, at the indicated temperature and strain rate. c refers to a craze pattern, s to a shear band pattern and cs to a combined craze and shear band pattern

Strain rate (min^{-1})	Temperature (°C)							
	20	30	40	50	60	70	80	90
0.01	c	c	c	c	c	cs	cs	s
0.1	c	c	c	c	c	c	c	c
1	c	c	c	c	c	c	c	c
10	c	c	c	c	c	c	c	c

range of test conditions both types of SAN exhibit both modes of deformation at the beads. The preference for craze or shear band formation depends on strain rate, temperature, copolymer composition and degree of interfacial adhesion. This is illustrated by Tables I to IV, where c refers to a craze pattern, s to a shear band pattern and cs to a combined craze and shear band pattern at the beads. It must be noted that the c to cs and cs to s transitions are not always as sharp as indicated. In Tables I to IV the deformation pattern observed at the vast majority of beads is given, but sometimes, under test conditions close to a transition, at a few beads the other pattern was observed.

A typical example of the combined craze and shear band pattern at an excellently adhering glass bead is shown in Fig. 1. In that case craze formation starts near the pole and shear band formation starts at 45° from the pole. Occasionally, shear bands also form at the tip of the crazes, which prevents further craze propagation (Fig. 2). It must be realized that the photographs shown in Figs. 1 and 2 were taken after unloading of the specimen. As a consequence of the elastic recovery which occurs on unloading, the angle the shear bands make to the tension direction is larger than 45°.

A typical example of the combined craze and shear band pattern at a poorly adhering glass bead is shown in Fig. 3. In contrast to an excellently adhering bead, the crazes and shear bands originate at the same location, namely at the tip of the interfacial crack formed upon dewetting. The formation of this combined pattern has been studied by microscopic *in situ* observation in the course of the tensile test. This was done at room temperature and at a low strain rate, in the same way as described elsewhere [5, 6]. It appeared that the shear bands are formed first and then, at the moment that shear deformation alone is apparently insufficient to achieve the imposed strain rate, the crazes are formed. As a matter of fact this sequence could already have been concluded from the deformation pattern shown in Fig. 3; if the crazes had been formed first, the shear bands would have been more likely to form at the tip of the crazes than at the bead because the maximum principal shear stress and the maximum distortion strain energy density would have been more likely to occur at the craze tip. It must again be realized that the photograph shown in Fig. 3 was taken after unloading of the specimen. Therefore, the angle the shear bands make to the tension direction is not 45° and the shadows at the poles of the bead, which are the indication of dewetting, are not visible [5, 6].

Tables I to IV show that for SAN an increasing temperature, a decreasing strain rate and an increasing wt % AN promote shear band formation at the expense of craze formation. A more

TABLE II Deformation pattern observed at poorly adhering glass beads in a SAN1 matrix

Strain rate (min^{-1})	Temperature (°C)							
	20	30	40	50	60	70	80	90
0.01	cs	cs	cs	cs	cs	cs	s	s
0.1	c	cs	cs	cs	cs	cs	cs	s
1	c	c	c	c	c	c	c	c
10	c	c	c	c	c	c	c	c

TABLE III Deformation pattern observed at excellently adhering glass beads in a SAN2 matrix

Strain rate (min^{-1})	Temperature (°C)							
	20	30	40	50	60	70	80	90
0.01	c	c	c	c	cs	cs	cs	s
0.1	c	c	c	c	c	c	cs	s
1	c	c	c	c	c	c	cs	cs
10	c	c	c	c	c	c	c	c

TABLE IV Deformation pattern observed at poorly adhering glass beads in a SAN2 matrix

Strain rate (min^{-1})	Temperature (°C)							
	20	30	40	50	60	70	80	90
0.01	cs	cs	s	s	s	s	s	s
0.1	cs	cs	cs	cs	cs	s	s	s
1	c	c	c	cs	cs	cs	s	s
10	c	c	c	c	cs	cs	s	s

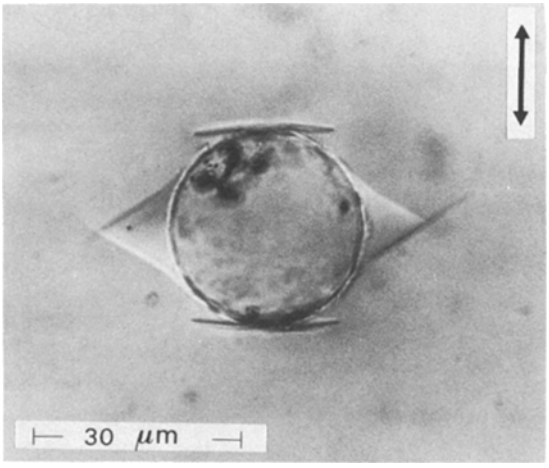

Figure 1 Combined craze and shear band pattern at an excellently adhering glass bead in a SAN matrix. The arrow indicates the direction of the applied tension.

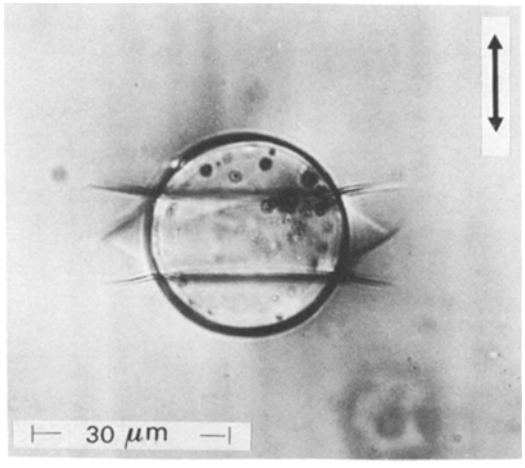

Figure 3 Combined craze and shear band pattern at a poorly adhering glass bead in a SAN matrix. The arrow indicates the direction of the applied tension.

striking result is that the degree of interfacial adhesion also affects the competition between craze and shear band formation, the latter being favoured at poorly adhering glass beads. For example, for SAN2 at a strain rate of $0.01\,min^{-1}$, in the case of poor adhesion a cs pattern is found from 20 to 30° C and the cs/s transition at 40° C (Table IV), whereas in the case of excellent adhesion a c pattern is found from 20 to 50° C, the c/cs transition at 60° C and the cs/s transition at 90° C (Table III). This effect can be understood by comparing the stress situation at the locations at which the crazes and shear bands form, as has been done in detail in a previous study [9]. At an excellently adhering glass bead, crazes form near the poles which are regions of maximum dilatation (sum of the three principal stresses). The dilatation in these regions is produced by three stresses because the stress state is triaxial here. At a poorly adhering glass bead both crazes and shear bands form at the tip of the interfacial crack. There the stress state is biaxial and the dilatation is therefore produced by only two stresses. As a result, the value of the dilatation is lower at the tip of the interfacial crack than at the pole of an excellently adhering bead, at least if the resistance to interfacial slip between the poorly adhering glass bead and the matrix is not too great (see Fig. 7, [9]). The values of the major principal shear stress and the distortion strain energy (which rule shear band formation), however, are not lower at the tip of the interfacial crack than at 45° from the pole of an excellently adhering bead. Thus the biaxiality of the stress field at the tip of the interfacial crack is unfavourable for the dilatation but not unfavourable for the major principal shear stress and the distortion strain energy, which accounts for the suppression of craze formation and its attendant promotion of shear band formation at poorly adhering glass beads.

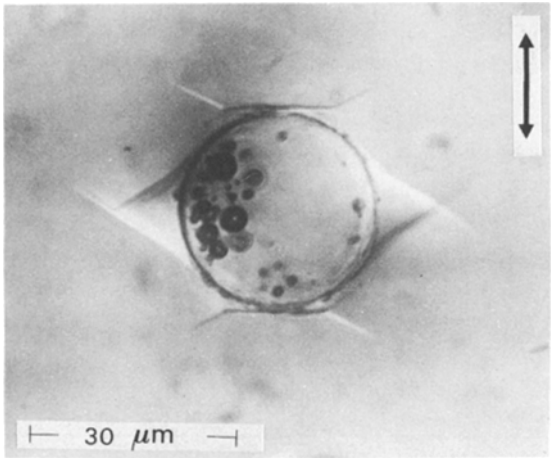

Figure 2 Combined craze and shear band pattern at an excellently adhering bead in a SAN matrix, showing shear band formation at the craze tips as well. The arrow indicates the direction of the applied tension. The spherical irregularities visible in the bead are air bubbles enclosed in the bead which are of no further importance.

Summarizing, in addition to matrix properties, strain rate and temperature, the stress

situation occurring locally within the material also determines the mode of tensile deformation, shear band formation being favoured under a biaxial stress state and craze formation under a triaxial stress state.

3.2. Kinetics of crazing and shear deformation

The light microscopic investigation of the previous section provides a good insight into the deformation processes that occur under certain test conditions. This makes it possible to study the kinetics of crazing and shear deformation under conditions for which it is well established that either crazing or shear deformation is the only non-Hookean deformation process. The kinetics of crazing have been studied by performing constant strain rate tensile tests with both PS–glass bead (90/10 vol %) and SAN1–glass bead (90/10 vol %) composites with excellent interfacial adhesion, in the temperature and strain rate range from 20 to 40° C and from 0.01 to 0.4 min^{-1}. The kinetics of shear deformation have been studied with the PC–glass bead (90/10 vol %) composite with excellent interfacial adhesion, in the temperature and strain rate range from 20 to 40° C and from 0.01 to 0.8 min^{-1}. The composites with poor interfacial adhesion have not been considered because for these composites, dewetting cavitation also contributes to the total non-Hookean deformation.

To study deformation kinetics under constant strain rate conditions, many authors take the yield point as the characteristic point and determine the dependence of the yield stress on strain rate and temperature. Under the present test conditions, however, the composites based on PS and SAN1 are rather brittle so that fracture occurs before the yield point is reached. To overcome this difficulty, the stress–strain ($\sigma - \varepsilon$) curves have been analysed according to the following simple model.

For a material in which one non-Hookean deformation process occurs, the total strain rate $d\varepsilon/dt$ can be described as [8, 10]:

$$\frac{d\varepsilon}{dt} = \frac{d\varepsilon_{el}}{dt} + \frac{d\varepsilon_p}{dt} \qquad (1)$$

where $d\varepsilon_{el}/dt$ and $d\varepsilon_p/dt$ are, respectively, the strain rates caused by elasticity and by the process. Assuming the amount of material that is deforming elastically to be constant during the entire tensile test, ε_{el} may be set equal to σ/E where E is the Young's modulus. Rearrangement of Equation 1 then gives:

$$\frac{d\varepsilon_p}{dt} = \frac{d\varepsilon}{dt}\left(1 - \frac{1}{E}\frac{d\sigma}{d\varepsilon}\right) \qquad (2)$$

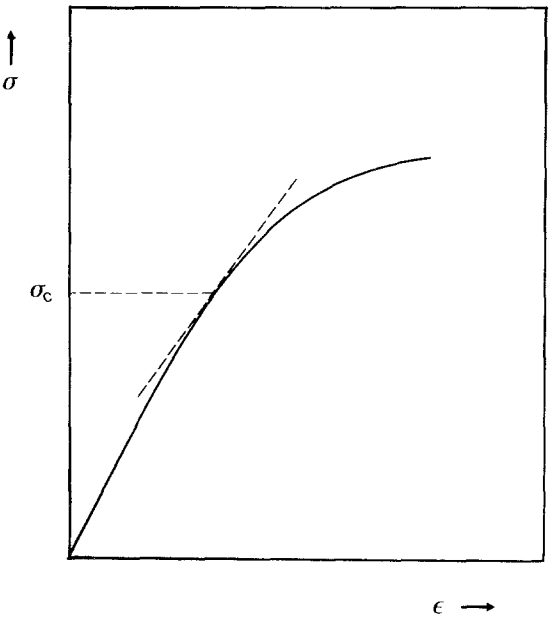

Figure 4 Determination of the stress σ_c at the characteristic point of the $\sigma-\varepsilon$ curve where $d\sigma/d\varepsilon = 0.75E$.

Now the $\sigma-\varepsilon$ curves have been analysed as illustrated in Fig. 4: the stress σ_c is determined at the point where the $\sigma-\varepsilon$ curve has a slope $d\sigma/d\varepsilon$ equal to $0.75E$, thus at the moment that the strain rate of the process amounts to 25% of the total strain rate. It should be noted that this characteristic point occurs at a relatively early stage of the tensile test. Therefore the assumption that up to this point the amount of material deforming elastically has not changed, is reasonable, and also the error made by taking σ_c as the engineering stress, i.e. without correction for the reduction in cross-sectional area of the specimen, is very small.

In Figs. 5 to 7 $d\varepsilon_p/dt$ is plotted logarithmically against the stress σ_c. The experimental data can be satisfactorily fitted to the Eyring equation for stress- and temperature-activated rate processes [7, 8]:

$$d\varepsilon_p/dt = 2A \exp\left(\frac{-\Delta H^*}{kT}\right) \sinh\left(\frac{\gamma V^* \sigma_c}{4kT}\right) \qquad (3)$$

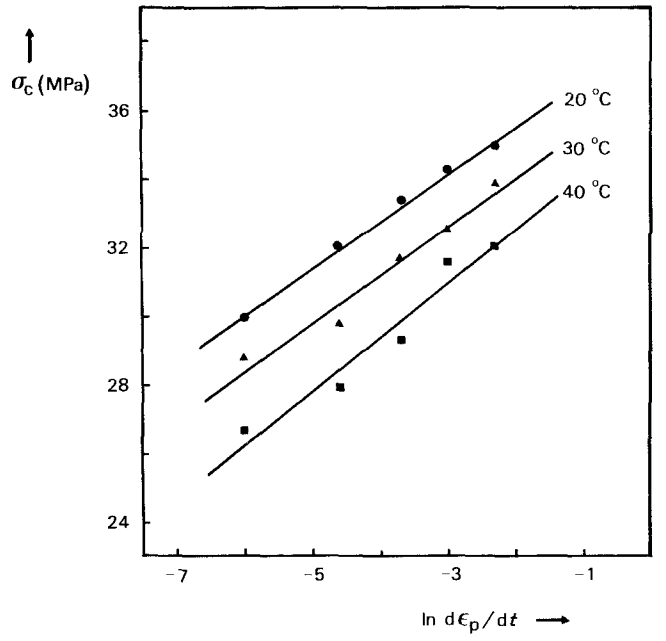

Figure 5 Dependence of σ_c on ln ($d\varepsilon_p/dt$) of the PS–glass bead (90/10 vol %) composite with excellent interfacial adhesion.

where A is a constant, ΔH^* is the activation enthalpy, V^* the activation volume, γ the stress concentration factor, k Boltzmann's constant, and T the absolute temperature. In the high-stress region where crazing and shear deformation occur, $2\sinh(\gamma V^*\sigma_c/4kT)$ is well approximated by $\exp(\gamma V^*\sigma_c/4kT)$.

The values of the Eyring parameters thus obtained are given in Table V. These are reasonable values that may be compared with values reported by other authors. For instance, for crazing in unfilled PS an activation enthalpy of 175 kJ mol^{-1} and an apparent activation volume of 5.6 nm^3 were reported [11, 12]. For crazing in polyethylene-toughened PS (with good interfacial adhesion) an activation enthalpy of

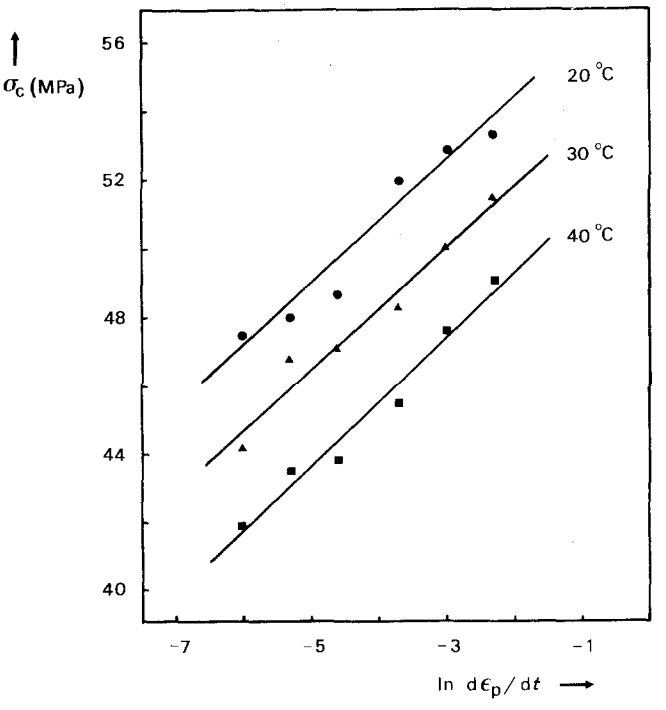

Figure 6 Dependence of σ_c on ln ($d\varepsilon_p/dt$) of the SAN1–glass bead (90/10 vol %) composite with excellent interfacial adhesion.

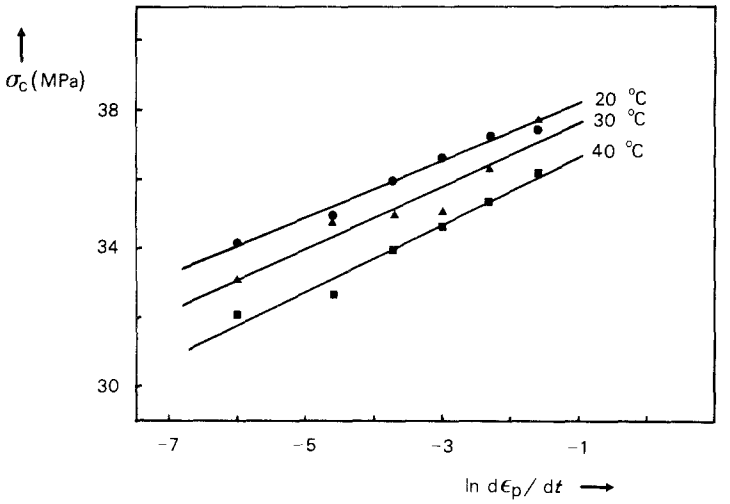

Figure 7 Dependence of σ_c on ln $(d\varepsilon_p/dt)$ of the PC–glass bead (90/10 vol %) composite with excellent interfacial adhesion.

280 kJ mol^{-1} and an apparent activation volume of 12 nm^3 were found, both values referring to the sum of areal craze growth and craze fibril growth [13]. For yielding in unfilled PC an activation enthalpy of 335 kJ mol^{-1} and an apparent activation volume of 11 nm^3 were reported [14].

The physical significance of the Eyring activation parameters for crazing and shear deformation is still obscure [3]. The molecular interpretation is hindered by the fact that the parameters generally refer to the overall rates of crazing and shear deformation, while these processes actually consist of a number of sub-processes. Crazing, for instance, can be divided into craze initiation, propagation and sometimes termination. The shear deformation in the PC–glass bead composite is even achieved by two completely different kinds of shear deformation, namely localized shear band formation at the glass beads and diffuse shearing of the remaining matrix material [15]. As a reasonable first attempt to interpret the value of ΔH^* for crazing in the PS–glass bead composite (195 kJ mol^{-1}), it may be compared with 230 kJ mol^{-1} for the activation energy for thermal bond rupture in PS [16]. The correspondence between these values suggest that chain scission may be the rate-determining step in crazing [12, 17]. The activation energy for thermal bond rupture in PC, however, amounts to 117 kJ mol^{-1} [18], which is considerably lower than the value of ΔH^* for shear deformation in the PC–glass bead composite (330 kJ mol^{-1}). This suggests that chain scission plays only a small, if any, part in the rate of shear deformation, and that shear deformation occurs by molecular flow of numerous monomeric units through the rupture of secondary bonds rather than primary ones.

4. Conclusion

An interesting result of the present study is that besides matrix properties, deformation rate and temperature, the nature of the stress concentrating heterogeneities also determines the mode of tensile deformation; the biaxial stress state

TABLE V Eyring parameters

Composite	Deformation mode	γV^* (nm^3)†	ΔH^* (kJ mol^{-1})	A (min^{-1})
PS–glass bead	crazing	20° C: 11.8(0.5)	195	4×10^{22}
		30° C: 11.9(1.1)		
		40° C: 11.1(1.5)		
SAN1–glass bead	crazing	20° C: 9.0(1.4)	160	3×10^{14}
		30° C: 9.3(0.7)		
		40° C: 9.1(0.9)		
PC–glass bead	shear deformation	20° C: 19.7(1.0)	330	2×10^{38}
		30° C: 18.4(2.1)		
		40° C: 17.8(1.3)		

† Figures in brackets are the standard deviations of the preceding figure.

induced by poorly adhering glass beads promotes "ductile" shear deformation at the expense of "brittle" crazing. This insight may be of interest in the development of new composite materials. By avoiding a triaxial stress state at the stress concentrators, a ductile response to tensile deformation might be achieved under test conditions that otherwise would yield a brittle response.

Acknowledgements

M. G. Kooy and G. T. C. Sanders are gratefully acknowledged for performing parts of the experimental work.

References

1. S. T. WELLINGHOFF and E. BAER, *J. Appl. Polym. Sci.* **22** (1978) 2025.
2. A. M. DONALD and E. J. KRAMER, *J. Mater. Sci.* **17** (1982) 1871.
3. A. J. KINLOCH and R. J. YOUNG, "Fracture Behaviour of Polymers" (Applied Science, London, 1983).
4. M. E. J. DEKKERS and D. HEIKENS, *J. Mater. Sci.* **18** (1983) 3281.
5. *Idem, J. Mater. Sci. Lett.* **3** (1984) 307.
6. *Idem, J. Mater. Sci.* **19** (1984) 3271.
7. H. EYRING, *J. Chem. Phys.* **4** (1936) 283.
8. A. S. KRAUSZ and H. EYRING, "Deformation Kinetics" (Wiley, New York, 1975).
9. M. E. J. DEKKERS and D. HEIKENS, *J. Mater. Sci.* **20** (1985) 3493.
10. D. HEIKENS, S. D. SJOERDSMA and W. J. COUMANS, *ibid.* **16** (1981) 429.
11. B. MAXWELL and L. F. RAHM, *Ind. Eng. Chem.* **41** (1949) 1988.
12. C. B. BUCKNALL, "Toughened Plastics" (Applied Science, London, 1977).
13. S. D. SJOERDSMA, M. E. J. DEKKERS and D. HEIKENS, *J. Mater. Sci.* **17** (1982) 2605.
14. C. BAUWENS-CROWET, J. C. BAUWENS and G. HOMÈS, *J. Polym. Sci. A2* **7** (1969) 735.
15. M. E. J. DEKKERS and D. HEIKENS, *J. Appl. Polym. Sci.* **30** (1985) 2389.
16. S. MADORSKY, *J. Res. Nat. Bur. Stand.* **62** (1959) 219.
17. S. N. ZHURKOV and E. E. THOMASHEVSKY, in "The Physical Basis of Yield and Fracture", Conference Proceedings (Institute of Physics, London, 1966) p. 200.
18. A. DAVIS and J. H. GOLDEN, *J. Chem. Soc.* **B1** (1968) 45.

Received 7 December 1984
and accepted 15 January 1985